Letter

Direct mass measurement of ^{93}Pd and implications for the isomer structures in ^{94}Ag: Tracing the two-proton decay branch

Gabriella Kripkó-Koncz,[1,2,3,*] Wolfgang R. Plaß,[1,4] Irene Dedes,[5] Duy Duc Dao,[6] Timo Dickel,[1,4] Christine Hornung,[1,2,4] Daler Amanbayev,[1,2,4] Samuel Ayet San Andrés,[1,4] Sönke Beck,[1,4] Julian Bergmann,[1] Andrey Blazhev,[7] Jerzy Dudek,[5,6,8] Hans Geissel,[1,4,†] Emma Haettner,[4] Nasser Kalantar-Nayestanaki,[9] Israel Mardor,[10,11] Ivan Miskun,[1] Ali Mollaebrahimi,[1,4,9] Xavier Mougeot,[12] Ivan Mukha,[4] Frédéric Nowacki,[6] Christoph Scheidenberger,[1,2,4] Juha Äystö,[13,14] Soumya Bagchi,[1,4,15,‡] Dimiter L. Balabanski,[16] Andrzej Baran,[8] Žiga Brenčič,[17] Volha Charviakova,[18] Paul Constantin,[16] Masoumeh Dehghan,[4] Abdelghafar Gaamouci,[5] Zhuang Ge,[4,13] Magdalena Górska,[4] Lizzy Gröf,[1] Oscar Hall,[3] Muhsin N. Harakeh,[9] Jan-Paul Hucka,[4,19] Anu Kankainen,[13,14] Ronja Knöbel,[4] Daria A. Kostyleva,[1,4] Natalia Kurkova,[20] Natalia Kuzminchuk,[4] Dragos Nichita,[16,21] Zygmunt Patyk,[18] Stephane Pietri,[4] Sivaji Purushothaman,[4] Moritz Pascal Reiter,[3] Mikael Reponen,[13,14] Heidi Roesch,[4,19] Anamaria Spătaru,[16,21] Goran Stanic,[22] Alexandru State,[16,21] Yoshiki K. Tanaka,[4] Matjaž Vencelj,[17] Helmut Weick,[4] Jie Yang,[23] Mikhail I. Yavor,[24] and Jianwei Zhao[4]

for the Super-FRS Experiment Collaboration

[1]*II. Physikalisches Institut, Justus-Liebig-Universität Gießen, D-35392 Gießen, Germany*

[2]*Helmholtz Research Academy Hesse for FAIR (HFHF), GSI Helmholtz Center for Heavy Ion Research, Campus Gießen, D-35392 Gießen, Germany*

[3]*School of Physics and Astronomy, University of Edinburgh, EH9 3FD Edinburgh, United Kingdom*

[4]*GSI Helmholtzzentrum für Schwerionenforschung GmbH, D-64291 Darmstadt, Germany*

[5]*Institute of Nuclear Physics Polish Academy of Sciences, PL-31 342 Kraków, Poland*

[6]*Université de Strasbourg, CNRS, IPHC UMR 7178, F-67 000 Strasbourg, France*

[7]*Institut für Kernphysik, Universität zu Köln, D-50937 Köln, Germany*

[8]*Institute of Physics, Marie Curie-Skłodowska University, PL-20 031 Lublin, Poland*

[9]*Nuclear Energy Group, ESRIG, University of Groningen, 9747 AA Groningen, The Netherlands*

[10]*School of Physics and Astronomy, Tel Aviv University, 6997801 Tel Aviv, Israel*

[11]*Soreq Nuclear Research Center, 81800 Yavne, Israel*

[12]*Université Paris-Saclay, CEA, List, Laboratoire National Henri Becquerel (LNE-LNHB), F-91120 Palaiseau, France*

[13]*Accelerator Laboratory, Department of Physics, University of Jyväskylä, FI-40014 Jyväskylä, Finland*

[14]*Helsinki Institute of Physics, FI-00014 Helsinki, Finland*

[15]*Department of Astronomy and Physics, Saint Mary's University, Halifax, Nova Scotia, Canada B3H 3C3*

[16]*Extreme Light Infrastructure-Nuclear Physics (ELI-NP), 077125 Bucharest-Măgurele, Romania*

[17]*Jožef Stefan Institute, SI-1000 Ljubljana, Slovenia*

[18]*National Centre for Nuclear Research, PL-02-093 Warszawa, Poland*

[19]*Institut für Kernphysik, Technische Universität Darmstadt, D-64289 Darmstadt, Germany*

[20]*Flerov Laboratory of Nuclear Reactions, JINR, 141980 Dubna, Russia*

[21]*Doctoral School in Engineering and Applications of Lasers and Accelerators, University Polytechnica of Bucharest, 060811 Bucharest, Romania*

[22]*Institut für Physik, Johannes Gutenberg-Universität Mainz, D-55099 Mainz, Germany*

[23]*School of Physics and Electronic Technology, Liaoning Normal University, 116029 Dalian, China*

[24]*Institute for Analytical Instrumentation, RAS, 190103 St. Petersburg, Russia*

(Received 13 November 2024; revised 22 June 2025; accepted 21 August 2025; published 23 October 2025)

The first direct mass measurement of ^{93}Pd, the one-proton-decay daughter of the (21^+) isomer in ^{94}Ag, has been performed, resulting in a mass excess value of −59 127(35) keV and reducing the mass uncertainty by an order of magnitude. As a consequence, the excitation energies of the presumed parent states of the one-proton (1p) decay and two-proton (2p) decay in ^{94}Ag are found to differ from each other by ten standard deviations. This shows that there is an incompatibility in the previously reported decay scheme of the 1p and 2p branches. Three scenarios are discussed, which could resolve this apparent contradiction, and elucidated by performing

*Contact author: gabriella.kripko-koncz@exp2.physik.uni-giessen.de

†Deceased.

‡Present address: Indian Institute of Technology (Indian School of Mines), Dhanbad, Jharkhand 826004, India.

state-of-the-art shell-model and mean-field calculations. The latter confirm that, based on the reported decay information, the 2p emission cannot be fed from the same (21^+) isomer as the 1p emission, but indicate that it could originate from a second, structurally different, high-spin state.

DOI: 10.1103/mhhn-kmgx

The silver isotope ^{94}Ag, containing 47 protons and 47 neutrons and located next to the proton dripline [1], has been reported to have a metastable state, a spin-trap isomer with spin and parity (21^+), which possesses properties that are unique throughout the entire Chart of the Nuclides: It has the highest spin observed so far for nuclei that live long enough to undergo β decay and a very high excitation energy of more than 6 MeV [2]. Even more intriguingly, it has been found to have multiple decay channels, such as β decay [3,4], β-delayed proton emission [5], direct one-proton (1p) decay [6,7], and even direct two-proton (2p) decay [8]. Correlations between the two emitted protons have been reported, which indicate that the 2p decay occurs via simultaneous 2p emission (true 2p decay), rather than via sequential 2p emission, although the latter should be energetically possible and would be expected to have a much larger branching ratio than the simultaneous 2p emission [8]. ^{94}Ag is thus the only known nucleus that has been reported to decay by both 1p and simultaneous 2p emission, and the only known nucleus with an odd number of protons to decay by simultaneous 2p emission [9,10]. The observation of 2p decay has been found exceedingly puzzling and has been questioned [7,11–13], giving rise to extended debate [14–19]. An experiment has been performed to verify the observation of 2p decay, but could reproduce only one of the two observed 1p decay branches, i.e., the one with the lower proton energy, denoted here as 1p(I) branch, and it did not see the 2p decay [7]. Despite further intense efforts [10,20–25], experimental as well as theoretical in nature, all attempts have failed so far to either consistently reconcile the observations with our understanding of nuclear structure or disprove them beyond doubt. Conversely, a successful explanation of the observed effects may reveal insights essential to the deeper understanding of the underlying quantum background driving these unique phenomena.

One method of validating the correctness of the reported decay scheme is to compare the energies of the 1p and 2p decay branches and thus to verify whether they indeed originate from the same parent state. Such a study has been performed previously, and a possible disagreement was pointed out [12]. However, at that time, the ground-state mass of the 1p decay daughter, ^{93}Pd, could be obtained only by a phenomenological extrapolation, thus preventing a final conclusion. In this Letter, the first direct mass measurement of the 1p decay daughter, ^{93}Pd, and a mass measurement of the 2p decay daughter, ^{92}Rh, are reported, and their impact on the 1p and 2p decay branches together with a detailed theoretical interpretation is discussed.

Neutron-deficient nuclides in the vicinity of ^{94}Ag were produced via projectile fragmentation at the fragment separator FRS [26] at GSI by impinging a ^{124}Xe primary beam with an energy of 790 MeV/nucleon and an intensity of approximately 1.2×10^9 ions per spill on a beryllium target with an areal density of 8045 mg/cm^2. The fragments were separated in flight in the FRS and delivered to the FRS Ion Catcher (FRS-IC) [27]. The FRS was operated in monochromatic mode with a monoenergetic degrader (735 mg/cm^2) at the central focal plane. In the FRS-IC, the fragments were slowed down in a second degrader and thermalized in a gas-filled cryogenic stopping cell (CSC) [28–30], from which they were extracted as singly charged ions and delivered to a multiple-reflection time-of-flight mass spectrometer (MR-TOF-MS) [31–33]. In the MR-TOF-MS, mass measurements were performed by confining the ions for a duration of 22 ms, and then ejecting them toward the detector, where the time of flight of the different ion species was recorded. For the measurements reported here, a mass resolving power of 700 000 (FWHM) was achieved.

The successful measurement of ^{93}Pd and, within the same setting, ^{92}Rh was only possible, because of two key approaches that were used for this experiment, but are applicable broadly at synchrotron facilities for many proton-rich nuclides. First, the use of a very thick target, in which multistep reactions can occur, enabled to significantly increase the production yields of the nuclides of interest. Second, to stop and measure several nuclides within the limited areal density of the CSC, usually several different degrader settings are needed, because the stopping range of an ion depends on its mass, charge state, and kinetic energy. For the region of the nuclear chart addressed in this experiment, however, the energy of the primary beam can be tuned such that isotones have the same range while maintaining the maximum stopping efficiency using the monochromatic mode of the FRS. The two $N = 47$ isotones, ^{93}Pd and ^{92}Rh, were stopped simultaneously in the CSC, and, because of the broadband capabilities [32,34] of the MR-TOF-MS, could be measured at the same time.

The data were analyzed following a proven procedure [34], which allows accurate determination of masses even in the case of a few events per ion species only [35,36]. The nuclide ^{93}Ru was used as a precision calibrant, with its mass taken from the AME2020 [37]. The resulting masses of ^{92}Rh and ^{93}Pd are reported in Table I. A detailed description of the experiment, data analysis, and results is provided in Ref. [38].

For ^{92}Rh, a mass excess of $-62\,989(10)$ keV was determined from the 85 detected events [Fig. 1(a)]. This value is in good agreement with previous Penning trap measurements [12,40,41]. The mass of the ^{93}Pd ground state was measured directly for the first time. The mass value reported in the AME2020 is from a β-decay end-point energy measurement [42]. In the present work, a mass excess of $-59\,127(35)$ keV was obtained from the nine detected events [Fig. 1(b)]. The obtained mass value agrees with the AME2020, but reduces the uncertainty by an order of magnitude. Notably, the

TABLE I. Measured mass excess (ME_{FRS-IC}) values for ^{92}Rh and ^{93}Pd compared with the literature values ME_{lit} [37]. $\Delta ME = ME_{FRS-IC} - ME_{lit}$ marks the deviation of the measured values from the literature.

Nuclide	Events	ME_{FRS-IC} (keV/c^2)	ME_{lit} (keV/c^2)	ΔME (keV/c^2)
^{92}Rh	85	−62 989(10)	−62 999(4)	10(11)
^{93}Pd	9	−59 127(35)	−58 980(370)	−147(372)

extrapolated mass value of ^{93}Pd used in the previous examination of the energies of the 1p and 2p decay branches [12] differs by almost two standard deviations from the present result.

Combining the newly measured mass excess of the 1p decay daughter, ^{93}Pd, the mass excess of hydrogen, ME(^{1}H) [37], the decay energy corresponding to the 1p(I) branch, $E_{1p,I} = 790(20)$ keV [6,7], and the excitation energy of the populated $(33/2^+)$ state in ^{93}Pd, $E_x(^{93}\text{Pd}, 33/2^+) = 4995.6(9)$ keV [43], gives a mass excess of the high-lying ^{94}Ag isomer of $ME(^{94}\text{Ag}, 21^+)_{1p,I} = -46\,050(40)$ keV. On the other hand, summing up the mass excess of the 2p decay daughter, ^{92}Rh, with $2 \times ME(^1\text{H})$, the 2p decay energy, $E_{2p} = 1900(100)$ keV [8], and $E_x(^{92}\text{Rh}, 11^+) = 1548.6(14)$ keV [44], the mass excess of the (21^+) isomer is determined to be $ME(^{94}\text{Ag}, 21^+)_{2p} = -44\,960(100)$ keV. These two alternative mass excess values of the (21^+) isomer differ by 1090(110) keV, i.e., by ten standard deviations (Fig. 2). This disagreement calls into question the experimental decay information [6,8]. Since the 1p(I) branch was confirmed [7], the 2p decay becomes the most debatable observation.

Using the new mass value of ^{93}Pd, the mass excess values of the presumed populated states in the 1p and 2p decay daughters, $ME(^{93}\text{Pd+p}, 33/2^+)$ and $ME(^{92}\text{Rh+2p}, 11^+)$, are the same within 21(37) keV (Fig. 2). Assuming that all decay branches originally reported in [6,8] are correct, a sequential 2p emission involving the $(33/2^+)$ state of ^{93}Pd and the (11^+) state of ^{92}Rh is energetically highly improbable. This would give an explanation for the observation in Ref. [8], where the reported correlations in the two emitted protons indicate a simultaneous 2p emission. However, this is potentially contradictory with the placement of the 1p and 2p decay branches suggested below as scenario (3) in this work (Fig. 2). To obtain the excitation energy from the mass excess of the (21^+) isomer, an accurate estimate of the ^{94}Ag ground-state mass is needed. In the literature, values from three different sources are available (Table II): first, from a linear fit to the Coulomb displacement energies (CDEs) for isobaric analog states (IASs) of odd-odd $N = Z$ nuclides with isospin $T = 1$ [12]; second, from a measurement of the Q_{EC} value of ^{94}Ag [42], the result of which was, however, listed as irregular in the AME2020; and third, from an extrapolation in the AME2020. Because of the large scatter of these three values, spanning almost 1 MeV, an independent estimate of the ^{94}Ag ground-state mass is called for. In the present work, it is derived from the global $\overline{\mathcal{F}t}$ value of the superallowed $0^+ \longrightarrow 0^+$ transitions [47] and the measured half-life of 27(2) ms [42,48,49] associated with the β decay of the ^{94}Ag $(0^+, T = 1)$ [50] ground state to the ^{94}Pd ground state, assuming a 100% branching ratio [47]. Though the general concept of the calculations is similar to Ref. [51], the main differences here are the incorporation of the transition-dependent radiative and nuclear-structure-related corrections [47] and the usage of the BetaShape code [52–54] for an accurate calculation of the statistical rate function. This $\overline{\mathcal{F}t}$-based approach results in a Q_{EC} value of 12 570(190) keV, which agrees within uncertainties with both Refs. [12,42], but differs by three standard

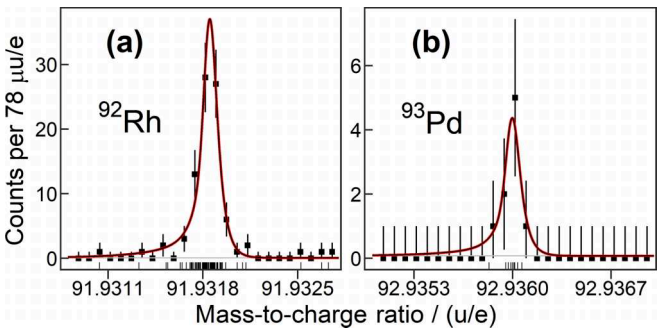

FIG. 1. Mass spectrum of (a) ^{92}Rh$^+$ ions and (b) ^{93}Pd$^+$ ions. The red lines represent the fits to the unbinned data ("rug" graph below the histogram) with a fixed hyper-EMG [39] peak shape (FWHM ≈ 120 keV), which was obtained from the peak of $^{12}C_3$ $^{19}F_3^+$ ions with ∼21 000 events.

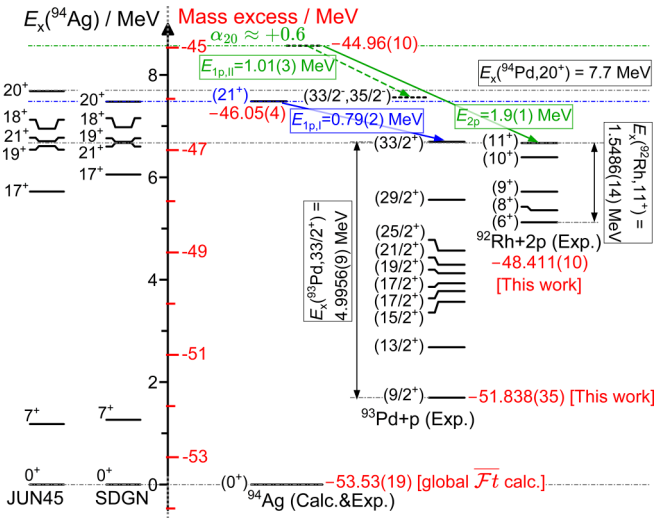

FIG. 2. Decay scheme according to the interpretation of this work, showing the discrepancy in the mass excess value of the ^{94}Ag (21^+) isomer when calculating it using the 1p- [6,7] and 2p-decay data [8], respectively. The black scale (left side) shows the ^{94}Ag level energies relative to its (0^+) ground state obtained by shell-model calculations, employing SDGN [45] and JUN45 [46] interactions, while the red scale (right side) shows the corresponding mass excess values resulting from our measurements. The mass of the ^{94}Ag ground state has been determined based on the $\overline{\mathcal{F}t}$ value.

TABLE II. Q_{EC} value and ME of the ^{94}Ag (0^+) ground state and excitation energy (E_x) of the (21^+) isomer(s) deduced in the present work via combining the measured masses of ^{93}Pd and ^{92}Rh, the 1p decay data [6,7], the 2p decay data [8], and either of the ^{94}Ag ground-state mass estimates.

^{94}Ag properties	$\overline{\mathcal{F}t}$ calculations (this work) (keV/c^2)	CDE systematics [12] (keV/c^2)	Indirect measurements [42] (keV/c^2)	AME2020 extrapolations [37] (keV/c^2)
$Q_{EC}(^{94}\text{Ag}, 0^+)$	12 570(190)	12 760(360)	$13\,350^{+690}_{-610}$	13 700(400)
$\text{ME}(^{94}\text{Ag}, 0^+)$	−53 530(190)	−53 340(360)	$-52\,750^{+690}_{-610}$	−52 400(400)
Independent from ^{94}Ag ground-state mass: $\text{ME}(^{94}\text{Ag}, 21^+)_{1p,I} = -46\,050(40)$ keV and $\text{ME}(^{94}\text{Ag}, 21^+)_{2p} = -44\,960(100)$ keV				
$E_x(^{94}\text{Ag}, 21^+)_{1p,I}$	7480(190)	7290(360)	6700^{+610}_{-690}	6350(400)
$E_x(^{94}\text{Ag}, 21^+)_{2p}$	8570(220)	8380(370)	7790^{+620}_{-700}	7440(410)

deviations from the extrapolated value given in AME2020 (Table II). While the $\overline{\mathcal{F}t}$-based Q_{EC} estimates, in general, follow a smooth trend for all odd-odd $N = Z$ nuclides up to $Z = 49$, the AME2020 extrapolations suggest a sudden change in the trend of Q_{EC} values by up to 1 MeV for odd-odd nuclides with $N = Z \geqslant 41$.

There are, in principle, three scenarios that could reconcile the observation of both 1p and 2p decays of ^{94}Ag as reported in Refs. [6,8] with the mass measurements reported here:

(1) The mass excess of the (21^+) isomer amounts to $\text{ME}(^{94}\text{Ag}, 21^+)_{1p,I} = -46\,050(40)$ keV, according to the 1p(I) decay branch [6,7] and the measured mass of ^{93}Pd. This suggests the 2p decay of the (21^+) isomer to feed a state in ^{92}Rh with the lower excitation energy of 450(110) keV and a lower spin instead of the previously reported (11^+) state [8]. However, no such state has been observed experimentally so far [42,44,55,56]. This makes scenario (1) rather unlikely.

(2) The mass excess of the (21^+) isomer amounts to $\text{ME}(^{94}\text{Ag}, 21^+)_{2p} = -44\,960(100)$ keV, according to the 2p decay data [8] and the measured mass of ^{92}Rh. This is only possible if the 1p(I) decay branch feeds a state in ^{93}Pd with a higher excitation energy, 6080(110) keV, compared to the previously reported ($33/2^+$) state [6]. The present experimental level scheme of ^{93}Pd [42,43,57] does not include a level at this energy, which makes also scenario (2) rather improbable. Moreover, the $T = 1$, (20^+) IAS in ^{94}Ag is expected to lie at the same excitation energy within ∼100 keV [58,59] as in ^{94}Pd, 7.7 MeV [4], the excitation energy of which has been further supported by the discovery of the (19^-) isomer in ^{94}Pd [60]. This is thought to give an upper limit for the excitation energy of the (21^+) spin-trap isomer to be able to explain the hindrance of the internal decay [4]. Using the $\overline{\mathcal{F}t}$-based or the CDE-based ^{94}Ag ground-state mass estimate, the (21^+) isomer in scenario (2), however, lies above this level (Fig. 2 and Table II). Thus, scenario (2) becomes even more unlikely.

(3) The 1p(I) and the 2p decay branches are fed from two separate isomeric states of ^{94}Ag with an excitation energy difference of 1090(110) keV as determined in this work (Fig. 2). The possibility of this scenario has been proposed in Ref. [19], but its scientific basis has, so far, not been examined. In this scenario, the complete experimental 1p and 2p decay information is consistent with the mass measurements reported here.

To further elucidate the three scenarios, shell-model and mean-field calculations have been performed. Large-scale shell model (LSSM) calculations were done in the $\pi\nu(gds)$ model space, comprising the $1g_{9/2}$, $1g_{7/2}$, $3s_{1/2}$, $2d_{5/2}$, and $2d_{3/2}$ orbitals for protons and neutrons, employing the SDGN effective interaction defined in Refs. [4,45,61], assuming a hypothetical ^{80}Zr core and allowing $14p14h$ excitations across the $N = Z = 50$ shell gap. The relevant states of ^{94}Ag predicted by the calculations are shown in Fig. 2. A 21^+ state is predicted at 6672 keV with a configuration involving $1g_{9/2}$ orbitals, $(\pi g_{9/2}^{-3} \nu g_{9/2}^{-3})_{21}$, preceded by a 17^+ state, thus successfully reproducing the spin-trap isomerism of the 21^+ state. The calculations also predict a 20^+ state at 7478 keV, which is the IAS with isospin $T = 1$ of the experimentally observed (20^+) state in ^{94}Pd [4]. No second high-spin isomer candidate is predicted within the $\pi\nu(gds)$ valence space. For comparison, shell-model calculations using the JUN45 interaction [46] were performed. The JUN45 gives an excellent agreement in the predicted level energies (Fig. 2), but in this case the order of the 21^+-19^+ states is swapped, showing the advantage of the SDGN interaction incorporating core excitations. To access the structure of the predicted 21^+ isomer and its associated nuclear deformation within the $\pi\nu(gds)$ valence space, the potential energy surface of ^{94}Ag 21^+ state was obtained using the discrete nonorthogonal shell model approach [61–63]. The calculations predict a nearly spherical shape with a slightly positive quadrupole deformation parameter of $\alpha_{20} < +0.1$ for the 21^+ state.

The mean-field calculations were performed employing the phenomenological, deformed Woods-Saxon Hamiltonian in its so-called universal parametrization [64,65]. The term "universal" signifies that the parameters are applicable to all nuclides in the Table of the Nuclides. Within the same theoretical framework, proton-emission lifetimes were deduced using the semiclassical Wentzel-Kramers-Brillouin (WKB) approximation [66]. Figure 3 shows the calculated proton single-nucleon energy spectrum for ^{94}Ag as a function of the quadrupole deformation parameter α_{20}. To enable proton emission, the emitting orbitals must have positive energies, and to fulfill the requirement to survive the production and measurement (>30 ms) [8,67], the WKB estimates suggest that their energy should be below 500 keV. Within this energy range, the most likely explanation for the angular momentum transfer of $9/2\,\hbar$ in the 1p(I) decay branch from the (21^+) isomer in ^{94}Ag to the ($33/2^+$) state in ^{93}Pd, while conserving the parity, necessarily involves the $1g_{9/2}$ orbital at $\alpha_{20} \approx +0.2$ (left yellow region in Fig. 3). However, at this deformation, there is no second orbital available to explain the total angular

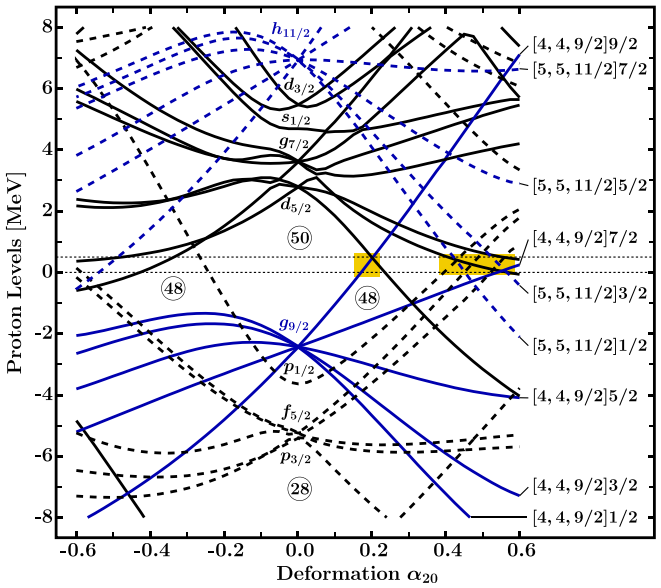

FIG. 3. Proton single-particle "universal" Woods-Saxon mean-field energies for ^{94}Ag as a function of the quadrupole deformation parameter α_{20}. The two orbitals playing decisive roles in the discussion of the proton emission, $1g_{9/2}$ (full lines) and $1h_{11/2}$ (dashed lines), are shown in blue color. The yellow areas mark the corresponding regions of interest with energies between 0 and 500 keV. The labels give the spherical labeling $[N, \ell, j]j_z$ for the dominating single-particle content.

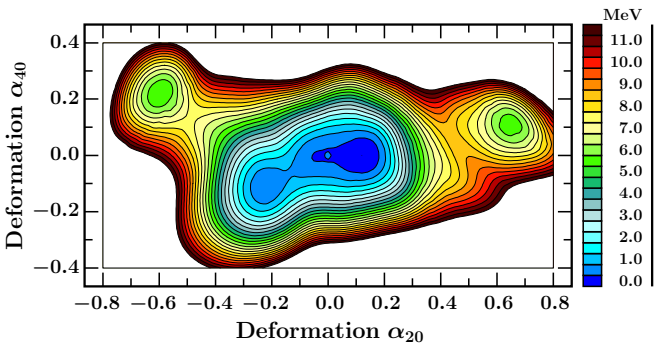

FIG. 4. Potential energy as a function of axially symmetric (appropriate for the spin isomer description) multipole deformation parameters (α_{20}, α_{40}) for ^{92}Pd, the even-even neighbor of ^{94}Ag. Note that in mean-field theory it has become a practical solution to investigate a nucleus with the help of the (lighter) even-even neighbor plus the respective single-particle orbitals, often giving close-lying results concerning the shape predictions.

momentum transfer of 10 $\hbar$ required for the 2p emission to the (11^+) state in ^{92}Rh, should it indeed originate from the same (21^+) state as the 1p emission. Therefore, a different state is required as a parent for the 2p emission, in agreement with scenario (3).

The spin and parity of the 2p-emission candidate are experimentally not known. Nevertheless, for the angular momentum transfer required for the 2p emission from a high-spin state in ^{94}Ag to the (11^+) state in ^{92}Rh, in Fig. 3 one can identify two orbitals with dominating $1h_{11/2}$ content or, alternatively, one orbital with dominating $1g_{9/2}$ content and one orbital with dominating $1h_{11/2}$ content as likely candidates. Both cases are found only at strongly elongated shapes with $\alpha_{20} \approx +0.4 \cdots +0.6$ (right yellow region in Fig. 3). While the prior configuration conserves parity under 2p emission, the latter configuration alters the parity.

The mean-field potential energy surface in Fig. 4 shows four local minima corresponding to possible axially symmetric configurations. The deformation of possible isomeric states can be obtained by a minimization of the sum of this potential energy and the particle-hole excitations that define the isomeric structures. Calculations show that the resulting quadrupole deformation α_{20} of the 1p(I)-emission candidate remains close to the valley that extends from about 0 to +0.2, in agreement with the LSSM results reported above, while the 2p-emission candidate can be associated with the minimum at $\alpha_{20} \approx +0.6$. This strong prolate deformation is in agreement with the deformation used in the model proposed in Ref. [8] to explain the 2p decay, the origin of which so far could not be understood [14].

Tilted Fermi surface calculations, similar to those in Refs. [68–71], predict a normal deformed prolate 21^+ state, the parent-state candidate for the 1p(I) branch, as a spin-trap isomer with $(\pi g_{9/2}^{-3} \nu g_{9/2}^{-3})_{21}$ configuration at an excitation energy of 7.77 MeV. The experimentally observed 7^+ isomer state [4,42] is also predicted as a spin-trap isomer in the same theoretical framework. For the 2p-emission candidate, no further quantitative results could be obtained. Its electromagnetic decay hindrance could be due to the fact that there are no (or very few) lower-energy superdeformed state candidates for such a decay, whereas the normal deformed states differ dramatically in terms of both the geometry and the particle-hole structures.

In Ref. [6], another 1p decay branch was observed with $E_{1p,II} = 1010(30)$ keV decay energy, denoted here as 1p(II) branch, and assigned to a daughter state with a tentative spin-parity assignment of $(33/2^-, 35/2^-)$ and a tentative placement in the level scheme of ^{93}Pd [42,43,57]. There is no orbital available in Fig. 3 to explain the presumed parity change of the 1p(II) branch, should it indeed originate from the same (21^+) isomer as the 1p(I) branch. Consequently, the two 1p branches should not stem from the same isomer. It is conceivable that the 1p(II) branch originates from the same superdeformed prolate isomer as the 2p emission (Fig. 2). Here, a negative-parity daughter state in ^{93}Pd can be realized in both possible 2p-emission configurations from a $1h_{11/2}$ or a $1g_{9/2}$ orbital for a positive- or negative-parity parent state, respectively.

The measured β half-life of 400(40) ms [3–5] should correspond mostly to the parent-state candidate for the 1p(I) branch [4], and thus the candidate for the 2p emission and the 1p(II) branch could have a much shorter lifetime, with the lower limit of about 30 ms [8,67]. This would explain the fact that only the 1p(I) decay branch could be experimentally confirmed in Ref. [7], but not the 2p and 1p(II) decay branches, since in this latter experiment a longer transport and measurement time of the nuclei (200–300 ms) [72] was used.

In summary, the first direct mass measurement of ^{93}Pd has been carried out, reducing the mass uncertainty by an order of magnitude. As a result, it is shown that the excitation

energies of the presumed parent states of the proposed 1p decay and 2p decay branches in ^{94}Ag disagree by ten standard deviations, which calls into question the reported decay scheme and, thus, also the observation of the 2p decay. Three different scenarios that could reconcile the 2p decay data with the present measurement are discussed and elucidated by performing state-of-the-art shell-model and mean-field calculations. The results of both calculations agree in the overlapping model spaces; i.e., they both predict a slightly prolate deformed 21^+ state as a spin-trap isomer, the 1p(I)-emission candidate. The mean-field calculations further show that, based on the reported decay information, the 2p emission cannot be fed from the same (21^+) isomer as the 1p(I) branch, but could stem from a strongly deformed high-spin isomer in ^{94}Ag, the single-particle configuration of which involves $1h_{11/2}$ intruder orbitals. As a consequence, possible explanations for several puzzles surrounding the 1p/2p decay branches of ^{94}Ag are provided, including the difference in the parent-state excitation energies, the origin of the strong prolate deformation of the 2p-emission candidate [8], and the nonobservation of the 1p(II) and 2p branches in a later experiment [7]. More experimental as well as theoretical evidence is needed for a final resolution, e.g., including the $1h_{11/2}$ orbitals in the shell-model valence space to examine whether the existence of a second high-spin isomer is supported in this framework, and mass measurements, decay and laser spectroscopy studies of the high-spin isomer(s) and their 1p/2p daughters [24,73].

Acknowledgments. The authors thank T. Eronen, G. Martínez-Pinedo, I. D. Moore, A. Sieverding, and V. Virtanen for valuable discussions. The experimental results reported here were obtained in the experiment S474, which was performed at the FRS at the GSI Helmholtzzentrum für Schwerionenforschung, Darmstadt (Germany) in the context of FAIR Phase 0 before 24 February 2022. This work was supported by the German Federal Ministry for Education and Research (BMBF) under Grants No. 05P19RGFN1, No. 05P21RGFN1, and No. 05P24RG4, by Justus-Liebig-Universität Gießen and GSI under the JLU-GSI strategic Helmholtz partnership agreement, by the German Research Foundation (DFG) under Grants No. 422761894 and No. AY 155/2-1, and by HGS-HIRe. Partial support is acknowledged from the French-Polish collaboration COPIN No. 04-113 and No. 23-157, from the Israel Ministry of Energy, Grant No. 220-11-052, from the Israel Science Foundation, Grant No. 2575/21, and from the international project PMW of the Polish Minister of Science and Higher Education, active during the period 2022–2024, Grant No. 5237/GSI-FAIR/2022/0. Z.G. acknowledges financial support from Research Council of Finland (previous Academy of Finland) Project No. 354589. A.K. acknowledges the support from the European Union's Horizon 2020 research and innovation program under Grant Agreement No. 771036 (ERC CoG MAIDEN).

Data availability. The data that support the findings of this article are not publicly available. The data are available from the authors upon reasonable request.

[1] I. Čeliković, M. Lewitowicz, R. Gernhäuser, R. Krücken, S. Nishimura, H. Sakurai, D. Ahn, H. Baba, B. Blank, A. Blazhev, P. Boutachkov, F. Browne, G. de France, P. Doornenbal, T. Faestermann *et al.*, New isotopes and proton emitters—crossing the drip line in the vicinity of ^{100}Sn, Phys. Rev. Lett. **116**, 162501 (2016).

[2] D. Abriola and A. A. Sonzogni, Nuclear data sheets for $A = 94$, Nucl. Data Sheets **107**, 2423 (2006).

[3] M. La Commara, K. Schmidt, H. Grawe, J. Döring, R. Borcea, S. Galanopoulos, M. Górska, S. Harissopulos, M. Hellström, Z. Janas, R. Kirchner, C. Mazzocchi, A. N. Ostrowski, C. Plettner, G. Rainovski *et al.*, Beta decay of medium and high spin isomers in ^{94}Ag, Nucl. Phys. A **708**, 167 (2002).

[4] C. Plettner, H. Grawe, I. Mukha, J. Döring, F. Nowacki, L. Batist, A. Blazhev, C. R. Hoffman, Z. Janas, R. Kirchner, M. La Commara, C. Mazzocchi, E. Roeckl, R. Schwengner, S. L. Tabor *et al.*, On the β-decaying (21^+) spin gap isomer in ^{94}Ag, Nucl. Phys. A **733**, 20 (2004).

[5] I. Mukha, L. Batist, E. Roeckl, H. Grawe, J. Döring, A. Blazhev, C. R. Hoffman, Z. Janas, R. Kirchner, M. La Commara, S. Dean, C. Mazzocchi, C. Plettner, S. L. Tabor, and M. Wiedeking, β-delayed proton decay of a high-spin isomer in ^{94}Ag, Phys. Rev. C **70**, 044311 (2004).

[6] I. Mukha, E. Roeckl, J. Döring, L. Batist, A. Blazhev, H. Grawe, C. R. Hoffman, M. Huyse, Z. Janas, R. Kirchner, M. La Commara, C. Mazzocchi, C. Plettner, S. L. Tabor, P. Van Duppen *et al.*, Observation of proton radioactivity of the (21^+) high-spin isomer in ^{94}Ag, Phys. Rev. Lett. **95**, 022501 (2005).

[7] J. Cerny, D. M. Moltz, D. W. Lee, K. Peräjärvi, B. R. Barquest, L. E. Grossman, W. Jeong, and C. C. Jewett, Reinvestigation of the direct two-proton decay of the long-lived isomer ^{94}Ag^m [0.4 s, 6.7 MeV, (21^+)], Phys. Rev. Lett. **103**, 152502 (2009).

[8] I. Mukha, E. Roeckl, L. Batist, A. Blazhev, J. Döring, H. Grawe, L. Grigorenko, M. Huyse, Z. Janas, R. Kirchner, M. La Commara, C. Mazzocchi, S. L. Tabor, and P. Van Duppen, Proton-proton correlations observed in two-proton radioactivity of ^{94}Ag, Nature (London) **439**, 298 (2006).

[9] M. Pfützner, I. Mukha, and S. Wang, Two-proton emission and related phenomena, Prog. Part. Nucl. Phys. **132**, 104050 (2023).

[10] F. Xing, J. Cui, Y. Wang, and J. Gu, Two-proton radioactivity of ground and excited states within a unified fission model, Chin. Phys. C **45**, 124105 (2021).

[11] O. L. Pechenaya, C. J. Chiara, D. G. Sarantites, W. Reviol, R. J. Charity, M. P. Carpenter, R. V. F. Janssens, T. Lauritsen, C. J. Lister, D. Seweryniak, S. Zhu, L.-L. Andersson, E. K. Johansson, and D. Rudolph, Level structure of ^{92}Rh: Implications for the two-proton decay of ^{94}Ag^m, Phys. Rev. C **76**, 011304 (2007).

[12] A. Kankainen, V.-V. Elomaa, L. Batist, S. Eliseev, T. Eronen, U. Hager, J. Hakala, A. Jokinen, I. D. Moore, Y. N. Novikov, H. Penttilä, A. Popov, S. Rahaman, S. Rinta-Antila, J. Rissanen *et al.*, Mass measurements and implications for the energy of the high-spin isomer in ^{94}Ag, Phys. Rev. Lett. **101**, 142503 (2008).

[13] D. G. Jenkins, Reviewing the evidence for two-proton emission from the high-spin isomer in ^{94}Ag, Phys. Rev. C **80**, 054303 (2009).

[14] K. Kaneko, Y. Sun, M. Hasegawa, and T. Mizusaki, Structure of upper-$g_{9/2}$-shell nuclei and shape effect in the ^{94}Ag isomeric states, Phys. Rev. C **77**, 064304 (2008).

[15] I. Mukha, H. Grawe, E. Roeckl, and S. Tabor, Comment on "Level structure of ^{92}Rh: Implications for the two-proton decay of ^{94}Ag^m", Phys. Rev. C **78**, 039803 (2008).

[16] O. L. Pechenaya, D. G. Sarantites, W. Reviol, C. J. Chiara, R. V. F. Janssens, C. J. Lister, and D. Seweryniak, Reply to "Comment on 'Level structure of ^{92}Rh: Implications for the two-proton decay of ^{94}Ag^m' ", Phys. Rev. C **78**, 039804 (2008).

[17] I. Mukha, E. Roeckl, H. Grawe, and S. Tabor, Comment on "Reviewing the evidence for two-proton emission from the high-spin isomer in ^{94}Ag", arXiv:1008.5346.

[18] A. Kankainen, Yu. N. Novikov, M. Oinonen, L. Batist, V.-V. Elomaa, T. Eronen, J. Hakala, A. Jokinen, P. Karvonen, M. Reponen, J. Rissanen, A. Saastamoinen, G. Vorobjev, C. Weber, and J. Äystö, Isomer and decay studies for the rp process at IGISOL, Eur. Phys. J. A **48**, 49 (2012).

[19] E. Roeckl and I. Mukha, Q values of radioactive decay: Examples from nuclear physics and related fields, Int. J. Mass Spectrom. **349-350**, 47 (2013).

[20] B. S. Nara Singh, T. S. Brock, R. Wadsworth, H. Grawe, P. Boutachkov, N. Braun, A. Blazhev, Z. Liu, M. Górska, S. Pietri, D. Rudolph, C. Domingo-Pardo, S. J. Steer, A. Ataç, L. Bettermann *et al.*, Influence of the np interaction on the β decay of ^{94}Pd, Phys. Rev. C **86**, 041301 (2012).

[21] M. Aggarwal, Proton radioactivity at non-collective prolate shape in high spin state of ^{94}Ag, Phys. Lett. B **693**, 489 (2010).

[22] J. Park, Decay spectroscopy of nuclei in the vicinity of ^{100}Sn, Ph.D. thesis, University of British Columbia, 2017.

[23] D. Lubos, Decay spectroscopy of ^{100}Sn and neighboring nuclei, Ph.D. thesis, Technische Universität München, 2016.

[24] M. Reponen, I. D. Moore, I. Pohjalainen, S. Rothe, M. Savonen, V. Sonnenschein, and A. Voss, An inductively heated hot cavity catcher laser ion source, Rev. Sci. Instrum. **86**, 123501 (2015).

[25] D.-X. Zhu, Y.-Y. Xu, H.-M. Liu, X.-J. Wu, B. He, and X.-H. Li, Two-proton radioactivity of the excited state within the Gamow-like and modified Gamow-like models, Nucl. Sci. Tech. **33**, 122 (2022).

[26] H. Geissel, P. Armbruster, K. Behr, A. Brünle, K. Burkard, M. Chen, H. Folger, B. Franczak, H. Keller, O. Klepper, B. Langenbeck, F. Nickel, E. Pfeng, M. Pfützner, E. Roeckl *et al.*, The GSI projectile fragment separator (FRS): A versatile magnetic system for relativistic heavy ions, Nucl. Instrum. Methods B **70**, 286 (1992).

[27] W. R. Plaß, T. Dickel, S. Purushothaman, P. Dendooven, H. Geissel, J. Ebert, E. Haettner, C. Jesch, M. Ranjan, M. Reiter, H. Weick, F. Amjad, S. Ayet, M. Diwisch, A. Estrade *et al.*, The FRS Ion Catcher—a facility for high-precision experiments with stopped projectile and fission fragments, Nucl. Instrum. Methods B **317**, 457 (2013).

[28] M. Ranjan, S. Purushothaman, T. Dickel, H. Geissel, W. R. Plaß, D. Schäfer, C. Scheidenberger, J. V. de Walle, H. Weick, and P. Dendooven, New stopping cell capabilities: RF carpet performance at high gas density and cryogenic operation, Europhys. Lett. **96**, 52001 (2011).

[29] S. Purushothaman, M. P. Reiter, E. Haettner, P. Dendooven, T. Dickel, H. Geissel, J. Ebert, C. Jesch, W. R. Plaß, M. Ranjan, H. Weick, F. Amjad, S. Ayet, M. Diwisch, A. Estrade *et al.*, First experimental results of a cryogenic stopping cell with short-lived, heavy uranium fragments produced at 1000 MeV/u, Europhys. Lett. **104**, 42001 (2013).

[30] M. Ranjan, P. Dendooven, S. Purushothaman, T. Dickel, M. Reiter, S. Ayet San Andrés, E. Haettner, I. Moore, N. Kalantar-Nayestanaki, H. Geissel, W. Plaß, D. Schäfer, C. Scheidenberger, F. Schreuder, H. Timersma *et al.*, Design, construction and cooling system performance of a prototype cryogenic stopping cell for the Super-FRS at FAIR, Nucl. Instrum. Methods Phys. Res. Sect. A **770**, 87 (2015).

[31] W. R. Plaß, T. Dickel, U. Czok, H. Geissel, M. Petrick, K. Reinheimer, C. Scheidenberger, and M. Yavor, Isobar separation by time-of-flight mass spectrometry for low-energy radioactive ion beam facilities, Nucl. Instrum. Methods B **266**, 4560 (2008).

[32] W. R. Plaß, T. Dickel, and C. Scheidenberger, Multiple-reflection time-of-flight mass spectrometry, Int. J. Mass Spectrom. **349–350**, 134 (2013).

[33] T. Dickel, W. R. Plaß, A. Becker, U. Czok, H. Geissel, E. Haettner, C. Jesch, W. Kinsel, M. Petrick, C. Scheidenberger, A. Simon, and M. I. Yavor, A high-performance multiple-reflection time-of-flight mass spectrometer and isobar separator for the research with exotic nuclei, Nucl. Instrum. Methods Phys. Res. Sect. A **777**, 172 (2015).

[34] S. Ayet San Andrés, C. Hornung, J. Ebert, W. R. Plaß, T. Dickel, H. Geissel, C. Scheidenberger, J. Bergmann, F. Greiner, E. Haettner, C. Jesch, W. Lippert, I. Mardor, I. Miskun, Z. Patyk *et al.*, High-resolution, accurate multiple-reflection time-of-flight mass spectrometry for short-lived, exotic nuclei of a few events in their ground and low-lying isomeric states, Phys. Rev. C **99**, 064313 (2019).

[35] C. Hornung, D. Amanbayev, I. Dedes, G. Kripko-Koncz, I. Miskun, N. Shimizu, S. Ayet San Andrés, J. Bergmann, T. Dickel, J. Dudek, J. Ebert, H. Geissel, M. Górska, H. Grawe, F. Greiner *et al.*, Isomer studies in the vicinity of the doubly-magic nucleus ^{100}Sn: Observation of a new low-lying isomeric state in ^{97}Ag, Phys. Lett. B **802**, 135200 (2020).

[36] A. Mollaebrahimi, C. Hornung, T. Dickel, D. Amanbayev, G. Kripko-Koncz, W. R. Plaß, S. Ayet San Andrés, S. Beck, A. Blazhev, J. Bergmann, H. Geissel, M. Górska, H. Grawe, F. Greiner, E. Haettner *et al.*, Studying Gamow-Teller transitions and the assignment of isomeric and ground states at $N = 50$, Phys. Lett. B **839**, 137833 (2023).

[37] W. J. Huang, M. Wang, F. G. Kondev, G. Audi, and S. Naimi, The AME 2020 atomic mass evaluation (I). Evaluation of input data, and adjustment procedures, Chin. Phys. C **45**, 030002 (2021); M. Wang, W. J. Huang, F. G. Kondev, G. Audi, and S. Naimi, The AME 2020 atomic mass evaluation (II). Tables, graphs and references, *ibid.* **45**, 030003 (2021).

[38] G. Kripkó-Koncz, Investigation of ground and isomeric states of exotic nuclei using advances in multiple-reflection time-of-flight mass spectrometry: Unraveling riddles surrounding the

proton-emitting isomer(s) in ^{94}Ag, Ph.D. thesis, Justus-Liebig-Universität Gießen, 2025.

[39] S. Purushothaman, S. Ayet San Andrés, J. Bergmann, T. Dickel, J. Ebert, H. Geissel, C. Hornung, W. R. Plaß, C. Rappold, C. Scheidenberger, Y. K. Tanaka, and M. I. Yavor, Hyper-EMG: A new probability distribution function composed of exponentially modified Gaussian distributions to analyze asymmetric peak shapes in high-resolution time-of-flight mass spectrometry, Int. J. Mass Spectrom. **421**, 245 (2017).

[40] C. Weber, V.-V. Elomaa, R. Ferrer, C. Fröhlich, D. Ackermann, J. Äystö, G. Audi, L. Batist, K. Blaum, M. Block, A. Chaudhuri, M. Dworschak, S. Eliseev, T. Eronen, U. Hager *et al.*, Mass measurements in the vicinity of the *rp*-process and the νp-process paths with the penning trap facilities JYFLTRAP and SHIPTRAP, Phys. Rev. C **78**, 054310 (2008).

[41] J. Fallis, J. A. Clark, K. S. Sharma, G. Savard, F. Buchinger, S. Caldwell, A. Chaudhuri, J. E. Crawford, C. M. Deibel, S. Gulick, A. A. Hecht, D. Lascar, J. K. P. Lee, A. F. Levand, G. Li *et al.*, Mass measurements of isotopes of Nb, Mo, Tc, Ru, and Rh along the νp- and *rp*-process paths using the Canadian Penning trap mass spectrometer, Phys. Rev. C **84**, 045807 (2011).

[42] J. Park, R. Krücken, D. Lubos, R. Gernhäuser, M. Lewitowicz, S. Nishimura, D. S. Ahn, H. Baba, B. Blank, A. Blazhev, P. Boutachkov, F. Browne, I. Čeliković, G. de France, P. Doornenbal *et al.*, New and comprehensive β- and βp-decay spectroscopy results in the vicinity of ^{100}Sn, Phys. Rev. C **99**, 034313 (2019).

[43] C. M. Baglin, Nuclear data sheets for $A = 93$, Nucl. Data Sheets **112**, 1163 (2011).

[44] C. M. Baglin, Nuclear data sheets for $A = 92$, Nucl. Data Sheets **113**, 2187 (2012).

[45] F. Nowacki, Shell model description of correlations in ^{56}Ni and ^{100}Sn, Nucl. Phys. A **704**, 223 (2002), RIKEN Symposium Shell Model 2000.

[46] M. Honma, T. Otsuka, T. Mizusaki, and M. Hjorth-Jensen, New effective interaction for f_5pg_9-shell nuclei, Phys. Rev. C **80**, 064323 (2009).

[47] J. C. Hardy and I. S. Towner, Superallowed $0^+ \rightarrow 0^+$ nuclear β decays: 2020 critical survey, with implications for V_{ud} and CKM unitarity, Phys. Rev. C **102**, 045501 (2020).

[48] P. Kienle, T. Faestermann, J. Friese, H.-J. Körner, M. Münch, R. Schneider, A. Stolz, E. Wefers, H. Geissel, G. Münzenberg, C. Schlegel, K. Sümmerer, H. Weick, M. Hellström, and P. Thirolf, Synthesis and halflives of heavy nuclei relevant for the *rp*-process, Prog. Part. Nucl. Phys. **46**, 73 (2001).

[49] K. Moschner, A. Blazhev, N. Warr, P. Boutachkov, P. Davies, R. Wadsworth, F. Ameil, H. Baba, T. Bäck, M. Dewald, P. Doornenbal, T. Faestermann, A. Gengelbach, J. Gerl, R. Gernhäuser *et al.*, Study of ground and excited state decays in $N \approx Z$ Ag nuclei, EPJ Web Conf. **93**, 01024 (2015).

[50] J. Jänecke and T. O'Donnell, Isospin inversion and n–p pairing in self-conjugate nuclei $A = 58$–98, Phys. Lett. B **605**, 87 (2005).

[51] T. Faestermann, R. Schneider, A. Stolz, K. Sümmerer, E. Wefers, J. Friese, H. Geissel, M. Hellström, P. Kienle, H.-J. Körner, M. Mineva, M. Münch, G. Münzenberg, C. Schlegel, K. Schmidt *et al.*, Decay studies of $N \approx Z$ nuclei from ^{75}Sr to ^{102}Sn, Eur. Phys. J. A **15**, 185 (2002).

[52] X. Mougeot, Reliability of usual assumptions in the calculation of β and ν spectra, Phys. Rev. C **91**, 055504 (2015).

[53] X. Mougeot, BetaShape: A new code for improved analytical calculations of beta spectra, EPJ Web Conf. **146**, 12015 (2017).

[54] X. Mougeot, Towards high-precision calculation of electron capture decays, Appl. Radiat. Isot. **154**, 108884 (2019).

[55] J. Park *et al.*, Properties of γ-decaying isomers and isomeric ratios in the ^{100}Sn region, Phys. Rev. C **96**, 044311 (2017).

[56] G. Häfner, K. Moschner, A. Blazhev, P. Boutachkov, P. J. Davies, R. Wadsworth, F. Ameil, H. Baba, T. Bäck, M. Dewald, P. Doornenbal, T. Faestermann, A. Gengelbach, J. Gerl, R. Gernhäuser *et al.*, Properties of γ-decaying isomers in the ^{100}Sn region populated in fragmentation of a ^{124}Xe beam, Phys. Rev. C **100**, 024302 (2019).

[57] G. Lorusso, A. Becerril, A. Amthor, T. Baumann, D. Bazin, J. S. Berryman, B. A. Brown, R. H. Cyburt, H. L. Crawford, A. Estrade, A. Gade, T. Ginter, C. J. Guess, M. Hausmann, G. W. Hitt *et al.*, β-delayed proton emission in the ^{100}Sn region, Phys. Rev. C **86**, 014313 (2012).

[58] M. A. Bentley, Excited states in isobaric multiplets—experimental advances and the shell-model approach, Physics **4**, 995 (2022).

[59] S. M. Lenzi, M. A. Bentley, R. Lau, and C. A. Diget, Isospin-symmetry breaking corrections for the description of triplet energy differences, Phys. Rev. C **98**, 054322 (2018).

[60] T. S. Brock *et al.* (RISING collaboration), Observation of a new high-spin isomer in ^{94}Pd, Phys. Rev. C **82**, 061309 (2010).

[61] A. Yaneva, S. Jazrawi, M. Mikolajczuk, M. Górska, P. Regan, B. Das, H. Albers, S. Alhomaidhi, T. Arici, A. Banerjee, G. Benzoni, B. Cederwall, M. Chishti, D. Dao, T. Davinson *et al.*, The shape of the $T_Z = +1$ nucleus ^{94}Pd and the role of proton-neutron interactions on the structure of its excited states, Phys. Lett. B **855**, 138805 (2024).

[62] D. D. Dao and F. Nowacki, Nuclear structure within a discrete nonorthogonal shell model approach: New frontiers, Phys. Rev. C **105**, 054314 (2022).

[63] M. Rocchini, P. E. Garrett, M. Zielińska, S. M. Lenzi, D. D. Dao, F. Nowacki, V. Bildstein, A. D. MacLean, B. Olaizola, Z. T. Ahmed, C. Andreoiu, A. Babu, G. C. Ball, S. S. Bhattacharjee, H. Bidaman *et al.*, First evidence of axial shape asymmetry and configuration coexistence in ^{74}Zn: Suggestion for a northern extension of the $N = 40$ island of inversion, Phys. Rev. Lett. **130**, 122502 (2023).

[64] The universal Woods-Saxon Hamiltonian and associated universal parametrisation have been developed in a series of articles: J. Dudek and T. Werner, New parameters of the deformed Woods-Saxon potential for $A = 110$–210 nuclei, J. Phys. G: Nucl. Phys. **4**, 1543 (1978); J. Dudek, A. Majhofer, J. Skalski, T. Werner, S. Cwiok, and W. Nazarewicz, Parameters of the deformed Woods-Saxon potential outside $A = 110$–210 nuclei, *ibid.* **5**, 1359 (1979); J. Dudek, W. Nazarewicz, and T. Werner, Discussion of the improved parametrisation of the Woods-Saxon potential for deformed nuclei, Nucl. Phys. A **341**, 253 (1980); J. Dudek, Z. Szymański, and T. Werner, Woods-Saxon potential parameters optimized to the high spin spectra in the lead region, Phys. Rev. C **23**, 920 (1981); S. Cwiok, J. Dudek, W. Nazarewicz, J. Skalski, and T. Werner,

Single-particle energies, wave functions, quadrupole moments and g-factors in an axially deformed Woods-Saxon potential with applications to the two-centre-type nuclear problems, Comput. Phys. Commun. **46**, 379 (1987).

[65] To illustrate the usage frequency of the universal Woods-Saxon Hamiltonian, the articles are quoted, which were published within the same year and the same journal and in which this Hamiltonian appeared: J. Rissanen, R. M. Clark, K. E. Gregorich, J. M. Gates, C. M. Campbell, H. L. Crawford, M. Cromaz, N. E. Esker, P. Fallon, U. Forsberg, O. Gothe, I.-Y. Lee, H. L. Liu, A. O. Machiavelli, P. Mudder *et al.*, Decay of the high-K isomeric state to a rotational band in ^{257}Rf, Phys. Rev. C **88**, 044313 (2013); W. Brodziński and J. Skalski, Predictions for superheavy elements beyond $Z = 126$, *ibid.* **88**, 044307 (2013); S. Lalkovski, A. M. Bruce, A. M. Denis Bacelar, M. Górska, S. Pietri, Z. Podolyák, P. Bednarczyk, L. Caceres, E. Casarejos, I. J. Cullen, P. Doornenbal, G. F. Farrelly, A. B. Garnsworthy, H. Geissel, W. Gelletly *et al.*, Submicrosecond isomer in $^{117}_{45}$Rh$_{72}$ and the role of triaxiality in its electromagnetic decay rate, *ibid.* **88**, 024302 (2013); H. L. Liu and F. R. Xu, Enhanced octupole correlation due to unpaired nucleons in actinide K-isomeric states, *ibid.* **87**, 067304 (2013); D. S. Delion and R. J. Liotta, Shell-model representation to describe α emission, *ibid.* **87**, 041302 (2013); D. S. Delion, R. J. Liotta, and R. Wyss, Simple approach to two-proton emission, *ibid.* **87**, 034328 (2013); D. S. Delion and J. Suhonen, Unified description of 2^+_1 states within the deformed quasiparticle random-phase approximation, *ibid.* **87**, 024309 (2013); D. Deleanu, D. L. Balabanski, T. Venkova, D. Bucurescu, N. Mărginean, E. Ganioğlu, G. Căta-Danil, L. Atanasova, I. Căta-Danil, P. Detistov, D. Filipescu, D. Ghiţă, T. Glodariu, M. Ivaşcu, R. Mărginean *et al.*, Excited states in ^{129}I, *ibid.* **87**, 014329 (2013).

[66] L. D. Landau and E. M. Lifshitz, Chapter VII—The quasi-classical case, in *Quantum Mechanics (Non-Relativistic Theory)*, 3rd ed., edited by L. D. Landau and E. M. Lifshitz (Pergamon Press, Oxford, 1977), p. 171.

[67] R. Kirchner, On the release and ionization efficiency of catcher-ion-source systems in isotope separation on-line, Nucl. Instrum. Methods B **70**, 186 (1992).

[68] M. Cerkaski, J. Dudek, Z. Szymański, C. G. Andersson, G. Leander, S. Aberg, S. G. Nilsson, and I. Ragnarsson, Nucleon binding in nuclei at high angular momentum, Phys. Lett. B **72**, 149 (1977).

[69] M. Cerkaski, J. Dudek, P. Rozmej, Z. Szymański, and S. G. Nilsson, Particle-hole structure of nuclear isomers at high angular momenta, Nucl. Phys. A **315**, 269 (1979).

[70] M. J. A. de Voigt, J. Dudek, and Z. Szymański, High-spin phenomena in atomic nuclei, Rev. Mod. Phys. **55**, 949 (1983).

[71] B. Liu, M. Brodeur, J. A. Clark, I. Dedes, J. Dudek, F. G. Kondev, D. Ray, G. Savard, A. A. Valverde, A. Baran, D. P. Burdette, A. M. Houff, R. Orford, W. S. Porter, F. Rivero *et al.*, Precise mass measurement of the longest odd-odd chain of nuclei with 1^+ ground states, Phys. Rev. C **111**, 034308 (2025).

[72] F. Blönnigen, D. Moltz, T. Lang, W. Knoll, X. Xu, M. Hotchkis, J. Reiff, and J. Cerny, Improvements to the helium-jet coupled on-line mass separator RAMA, Nucl. Instrum. Methods B **26**, 328 (1987).

[73] M. Reponen, R. P. de Groote, L. Al Ayoubi, O. Beliuskina, M. L. Bissell, P. Campbell, L. Cañete, B. Cheal, K. Chrysalidis, C. Delafosse, A. Roubin, C. S. Devlin, T. Eronen, R. F. Garcia Ruiz, S. Geldhof *et al.*, Evidence of a sudden increase in the nuclear size of proton-rich silver-96, Nat. Commun. **12**, 4596 (2021).